

Ultrasonic image reconstruction via plane wave stacking

F. Natterer

Institut für Numerische und Angewandte Mathematik

Westf. Wilhelms-Universität Münster

Einsteinstrasse 62, D-48149 Münster, Germany

e-mail: nattere@math.uni-muenster.de

July 6, 2005

1 Introduction

Plane wave stacking is a method for synthesizing from actually measured physical data, the data that would result from plane wave illumination of an object. This technique has been used in seismic imaging ever since it was invented by [1] in 1978; see [2] for a more recent reference.

To fix ideas let us consider the following seismic imaging problem. Let $c(x)$, $x \in \mathbb{R}^n$ be the speed of sound in the subsurface $x_n > 0$. Assume the seismogram $u_s(x', 0, t)$ is measured for $x' \in \mathbb{R}^{n-1}$, $t \geq 0$ and all sources $s \in \mathbb{R}^{n-1}$ where u is the solution of

$$\frac{\partial^2 u_s}{\partial t^2} = c^2 \Delta u_s \quad \text{in } x_n > 0, \quad t \geq 0, \quad (1.1)$$

$$\frac{\partial u_s}{\partial x_n} = p(x' - s)q(t) \quad \text{on } x_n = 0, \quad t \geq 0, \quad (1.2)$$

$$u_s = 0 \quad \text{for } t < 0 \quad (1.3)$$

with p, q modelling the exciting impulse. In the language of seismic imaging $g_s = u_s(\cdot, 0, \cdot)$ is referred to as common source gather. Common shot gathers

are a standard way of collecting seismic data; see e. g. [4].

Common shot gathers can be turned into plane wave data by the following (obvious) procedure. To fix ideas consider the case $n = 2$. Then

$$g_s(x_1, t) = u_s(x_1, 0, t), x_1 \in \mathbb{R}^1, t \geq 0 \quad (1.4)$$

is the usual seismogram. Let $\alpha, |\alpha| < \pi/2$ be an angle, and let

$$g_\alpha(x_1, t) = \int_{\mathbb{R}^1} g_s(x_1, t - \frac{s}{c} \sin \alpha) ds. \quad (1.5)$$

g_α is the value at $x_2 = 0$ of the solution

$$u_\alpha(x, t) = \int_{\mathbb{R}^1} u_s(x, t - \frac{s}{c} \sin \alpha) ds \quad (1.6)$$

of (1.1) that exhibits a wave front making an angle α with the surface $x_2 = 0$. Thus using g_α as data set has the same effect as insonifying the subsurface with a plane wave making an angle α with the surface.

In the next section we see that two plane waves making an angle of $\pi/2$ with one another suffice to determine an object in the subsurface - at least in the Born approximation - completely. Thus, using (1.5) with $\alpha = \pm\pi/4$ is enough to image the subsurface. In section we show that by the propagation-backpropagation algorithm applied to (1.5) for $\alpha = \pm\pi/4$ faithful reconstructions can be obtained for strongly scattering objects. We demonstrate the efficacy of this method by way of the Marmousi data [6].

The propagation-backpropagation algorithm is by no means new. It is just another example of the popular adjoint method [7] and reduces in the case of the wave equation to consecutive time reversal [8]. It has been used extensively by Sielschott [9], [10] for furnace imaging problems. Migration methods in seismic imaging can be viewed as the first step of an adjoint method [11].

The new aspect of this paper lies in the combination of propagation-backpropagation with plane wave stacking as described in (1.5). Using adjoint methods directly on the common source gathers is too time consuming, since propagation and backpropagation have to be done for each source, leading to a greedy algorithm. Applying propagation-backpropagation to the stacked

data (1.5) is doable since it has to be done for two data sets $\alpha = \pm\pi/4$ only. The complexity of the combined method corresponds to the complexity of the well known and widely used ART algorithm of computerized tomography [12].

2 The Born approximation for plane waves

In the following we assume the object to be illuminated by a plane wave falling in in the x_n -direction:

$$\begin{aligned}\frac{\partial^2 u}{\partial t^2} &= c^2 \Delta u && \text{in } x_n > 0, \quad t \geq 0 \\ \frac{\partial u}{\partial x_n} &= q(t) && \text{on } x_n = 0, \quad t \geq 0 \\ u &= 0 && \text{for } t < 0.\end{aligned}\tag{2.1}$$

Further we assume that

$$c^2 = c_0^2 / (1 + f)$$

with f sufficiently small. Let u_0 be the solution of (2.1) with $f = 0$ and let $v = u - u_0$. Then,

$$\begin{aligned}\frac{\partial^2 v}{\partial t^2} &= c_0^2 \Delta v - f \frac{\partial^2 u}{\partial t^2} && \text{in } x_n > 0, \quad t \geq 0, \\ \frac{\partial v}{\partial x_n} &= 0, && \text{on } x_n = 0, \quad t \geq 0, \\ v &= 0 && \text{for } t < 0.\end{aligned}\tag{2.2}$$

The Born approximation is obtained by replacing u in (2.2) by u_0 . Thus,

$$\begin{aligned}\frac{\partial^2 v}{\partial t^2} &= c_0^2 \Delta v - f \frac{\partial^2 u_0}{\partial t^2} && \text{in } x_n > 0, \quad t \geq 0, \\ \frac{\partial v}{\partial x_n} &= 0, && \text{on } x_n = 0, \quad t \geq 0, \\ v &= 0 && \text{for } t < 0.\end{aligned}\tag{2.3}$$

Fourier transforming with respect to t we obtain with $k = \frac{\omega}{c_0}$

$$\begin{aligned}\Delta \hat{v} + k^2 \hat{v} &= -k^2 f \hat{u}_0, \quad x_n > 0, \\ \frac{\partial \hat{v}}{\partial x_n} &= 0, \quad x_n = 0.\end{aligned}$$

Since v vanishes for $t < 0$, \hat{v} satisfies the Sommerfeld radiation condition as $|x| \rightarrow \infty$, $x_n > 0$. Hence, with G_k the free space Green's function, we have

$$\hat{v}(x, \omega) = \frac{k^2}{2} \int_{\mathbb{R}^n} G_k(x - y) (f \hat{u}_0)(y', |y_n|) dy.$$

Thus we have for the Fourier transformed seismogram

$$\hat{v}(x', 0, \omega) = \frac{k^2}{2} \int_{\mathbb{R}^n} G_k(x' - y', y_n) (f \hat{u}_0)(y', |y_n|) dy. \quad (2.4)$$

Inserting

$$\hat{u}_0(x, a) = e^{ikx_n} \hat{q}(\omega)$$

yields

$$\hat{v}(x', 0, \omega) = k^2 \hat{q}(\omega) \int_{y_n > 0} G_k(x' - y', y_n) f(y', y_n) e^{iky_n} dy.$$

Making use of the plane wave decomposition of G_k , i. e.

$$G_k(x) = ic_n \int_{\mathbb{R}^{n-1}} e^{i(|x_n|a(z) - x' \cdot z)} \frac{dz}{a(z)}$$

with $c_n = 1/4\pi$, $c_3 = 1/8\pi^2$ (see e.g. [3], p. 49) we obtain

$$\begin{aligned}\hat{v}(x', 0, \omega) &= ik^2 c_n \hat{q}(\omega) \int_0^\infty \int_{\mathbb{R}^{n-1}} \int_{\mathbb{R}^{n-1}} e^{i(y_n a(z) - (x' - y') \cdot z)} dz f(y', y_n) e^{iky_n} dy' dy_n \\ &= ik^2 c_n \hat{q}(\omega) (2\pi)^{n/2} \int_{\mathbb{R}^{n-1}} e^{-ix' \cdot z} \hat{f}(-z, -k - a(z)) dz.\end{aligned}$$

Doing a $(n - 1)$ dimensional Fourier transform with respect to x' yields

$$\hat{\hat{v}}(z, 0, \omega) = ik^2 c_n \hat{q}(\omega) (2\pi)^{n-1/2} \hat{f}(z, -k - a(z)). \quad (2.5)$$

$\hat{\hat{v}}$ is the Fourier transform in t and x_1 of v , i.e. the 2 D Fourier transform of the seismogram. Thus $\hat{f}(\xi)$ is determined by the data - within the Born approximation - on the arc $\xi_n = -k - a(\xi')$, $|\xi'| \leq k$. If we let k vary between k_0 and k_1 and assuming f to be real we obtain \hat{f} in the hatched region in Fig. 1.

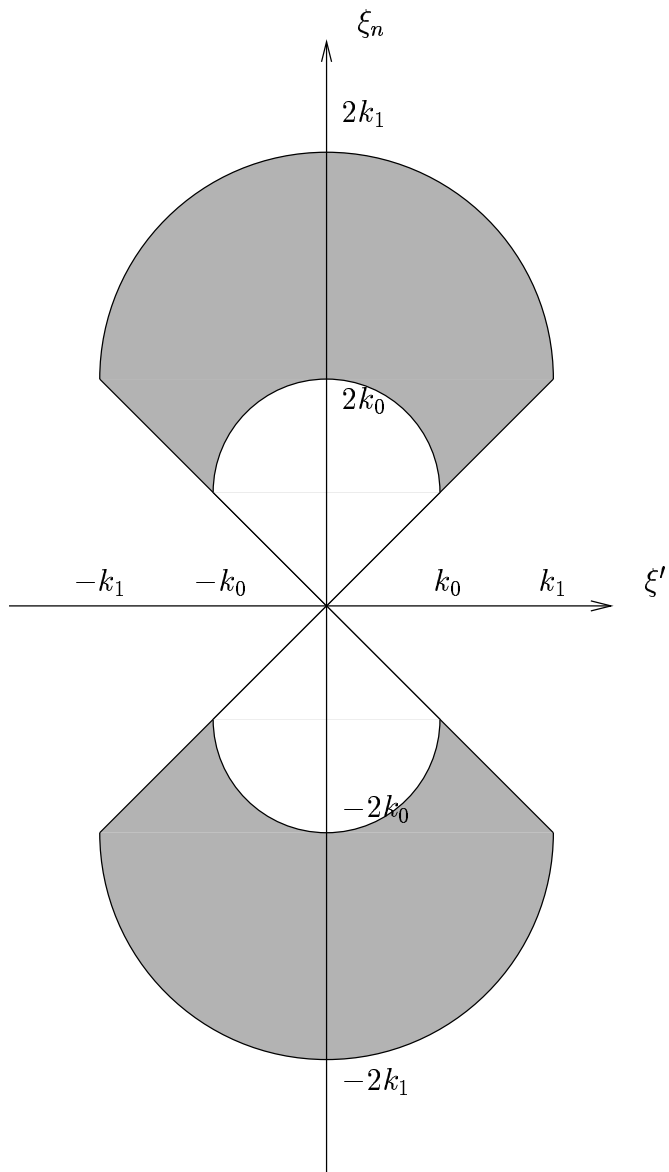


Fig. 1: The Fourier transform of f is determined in the hatched area

The range (k_0, k_1) of available wave numbers depends entirely on the source wavelet q . For $q = \delta$, the Dirac δ -function, $k_0 = 0$ and $k_1 = \infty$. In this case we conclude from Fig. 1 that a layered medium with dip angle $< \pi/4$ can be well reconstructed by a single downgoing plane wave, and that an arbitrary medium can be reconstructed from two plane waves making an angle of $\pi/2$. In view of [5] this is not surprising. Unfortunately such a wavelet is not supported by the earth. For real wavelets, such as the Ricker wavelet, the range of usable wave-numbers is restricted to a finite interval (k_0, k_1) . Typically, $k_0 = k_1/10$. In that case the part $|\xi| < k_0$ of $\hat{f}(\xi)$ can not be recovered, not even from plane waves of arbitrary directions.

3 The *PBP* algorithm in time domain

In the following we describe the *PBP* algorithm in time domain for an arbitrary set of incoming waves. In the context of the present paper the set would consist of two approximate plane waves making an angle of $\pm 45^\circ$ with the surface $x_n = 0$, being synthesized by suitable stacking of common source gathers.

Let $g_p(x', t)$, $p = 1, \dots, P$ be the seismogram for the p -th incoming plane wave, and let u_p be the corresponding field. Then,

$$\begin{aligned} \frac{\partial^2 u_p}{\partial t^2} &= c^2 \Delta u_p & \text{in } & x_n > 0, 0 \leq t \leq T, \\ \frac{\partial u_p}{\partial x_n} &= g_p(x', t) & \text{on } & x_n = 0, 0 \leq t \leq T, \\ u_p &= 0 & \text{for } & t < 0. \end{aligned} \tag{3.1}$$

The problem is to recover $c^2 = c_0^2/(1 + f)$ from g_p , $p = 1, \dots, P$.

We rewrite (3.1) as

$$R_p(f) = g_p, \quad p = 1, \dots, P$$

where the nonlinear map R_p is defined by

$$(R_p(f))(x', t) = u_p(x', 0, t)$$

with u_p the solution of (3.1). The differentiability of R_p has been settled in [13]. With an appropriate choice of spaces we have for the Fréchet-derivative R'_p of R_p

$$(R'_p(f)h)(x', t) = w(x', 0, t)$$

where w is the solution of

$$(1 + f) \frac{\partial^2 w}{\partial t^2} = c_0^2 \Delta w - h \frac{\partial^2 u_p}{\partial t^2} \quad \text{in } x_n > 0, 0 \leq t \leq T,$$

$$\frac{\partial w}{\partial x_n} = 0 \quad \text{on } x_n = 0, 0 \leq t \leq T,$$

$$w = 0 \quad \text{for } t < 0.$$

We also need the adjoint of $R'_p(f)$. We have (see [7])

$$(R'(f)^*g)(x) = \int_0^T Z(x, t) \frac{\partial^2 u_p}{\partial t^2}(x, t) dt \quad (3.2)$$

where Z is the solution of

$$(1 + f) \frac{\partial^2 Z}{\partial t^2} = c_0^2 \Delta Z \quad \text{in } x_n > 0, \quad 0 \leq t \leq T \quad (3.3)$$

$$(3.4)$$

$$\frac{\partial Z}{\partial x_n} = g \quad \text{on } x_n = 0, \quad 0 \leq t \leq T, \quad (3.5)$$

$$(3.6)$$

$$Z = 0 \quad \text{for } t > T. \quad (3.7)$$

The *PBP* algorithm now reads

$$f \leftarrow f - \beta R'_p(f)^*(R_p(f) - g_p) \quad (3.8)$$

where p runs through the integers $1, \dots, P$ in a suitable fashion. As in the ART algorithm of CT (see e.g. [12]) the choice of p and of the relaxation parameter β are crucial. We favour a random choice of p ; see [3]. At the present stage of our work, β is chosen by trial and error.

4 Reconstruction of the Marmousi data set

In this section we report on our experiences with the Marmousi model [6]. This is a 385 x 122 array of velocities c , ranging from 1500 m/s to 5500 m/s, mapping an area 9 km long and 3 km deep. Since c has a pronounced linear trend in depth we normalized the original Marmousi data $marm(x, z)$, putting

$$\sqrt{1 + f(x, z)} = \frac{c_0 + (c_1 - c_0)z/d}{marm(x, z)}, \quad 0 \leq z \leq d \quad (4.1)$$

where $d = 3$ km, $c_0 = 1500$ m/sec, $c_1 = 3500$ m/s. With these settings the function f varies between -0.727 and 0.635 , see Fig. 2a.

We generated data by solving (1.1,1.2,1.3) by a finite difference method in dimension $n = 2$. We chose

$$p(x_1) = e^{-2(x_1/\Delta s)^2}, \quad (4.2)$$

$$q(t) = e^{-(t/\tau)^2/2} \quad (4.3)$$

with $\Delta s = 0.25$ km the source distance and $\tau = 0.06$ s. The sources are sitting at the surface $z = 0$. From these data it is possible to generate plane wave data by the stacking procedure described in section 1. Equivalently (and much more efficiently) we can solve (1.1), (1.3) with the boundary conditions

$$\frac{\partial u}{\partial x_2}(x_1, 0, t) = \sum_{l=0}^L p(x_1 - l\Delta s)q(t - \sin(\alpha)l\Delta s/c_0) \quad (4.4)$$

and

$$\frac{\partial u}{\partial x_2}(x_1, 0, t) = \sum_{l=0}^L p(x_1 - (L - l)\Delta s)q(t - \sin(\alpha)(L - l)\Delta s/c_0), \quad (4.5)$$

for the plane waves coming in from left and right, respectively, making angles of $\pm\alpha$ with the surface. We know from the analysis in section 2 that the two plane waves with angles $\pm\pi/4$ suffice to determine f uniquely.

For solving the forward problem in the *PBP* algorithm we used the same boundary conditions (4.4, 4.5) in each of the equation $g_p = R_p f$, $p = 1, 2$, p referring to the angles $\pi/4$, $-\pi/4$, respectively. Solving the adjoint system (3.2) can be done independently of p .

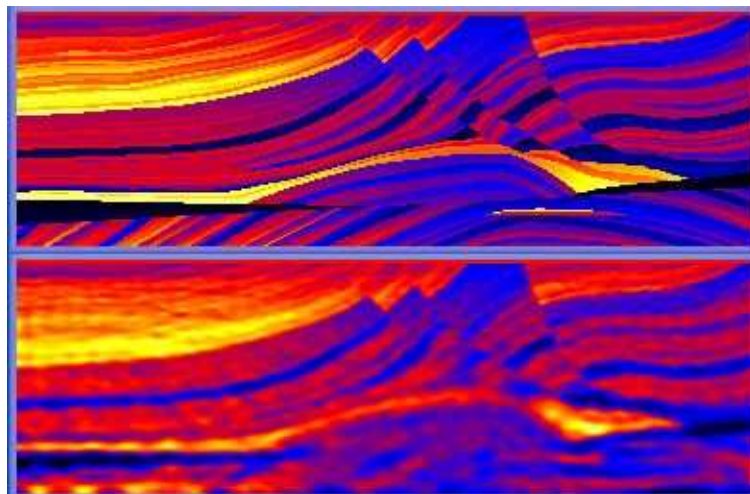


Fig. 2: (a) top: Marmousi velocity model
 (b) bottom: Reconstruction of Marmousi velocity model

In Fig. 2 (b) we display the reconstruction obtained after 100 steps with $\beta = 0.1$. The computing time was 2 minutes on a 3 GHz double processor PC. Our result is clearly competitive with others, e.g. the one in [14]. However the success of our method depends entirely on the choice (4.3) of the source wavelet q : The spectrum of q has to include the frequency 0. For the wavelets that are used in practice, e.g. for the Ricker wavelet, this is not the case. Using our algorithm for such a wavelet produces results that are useless: The velocities are wrong, and the layers are visible but at the wrong place.

Acknowledgement: We would like to thank Marcel Zwaan, Shell EPE, for explaining to us the technical details of seismic imaging.

5 Transmission measurements

So far we used only reflected signals, i.e. sources and receivers are sitting on the same side of the object to be imaged. If receivers can be put on the opposite side we can make transmission measurements. This is the case in industrial imaging [9] and medical imaging [15]. We will see that transmission measurements permit the reconstruction of the low frequency part of f even for source wavelets that do not have low frequencies.

The analysis parallels the one for reflection. Our data function is now $g_s = u_s(\cdot, r, \cdot)$ where $r > 0$ and f is supported in $0 \leq x_n \leq r$. In the Born approximation we obtain instead of (2.4)

$$\hat{v}(z, r, \omega) = ik^2 c_n \hat{q}(\omega) e^{ir a(z)} (2\pi)^{n-1/2} \hat{f}(z, -k + a(z)) \quad (5.1)$$

$\hat{f}(\xi)$ is now determined on the arc $\xi_n = -k + a(\xi')$, $|\xi'| \leq k$. If we let vary k between k_0 and k_1 and assuming f to be real we obtain \hat{f} in the hatched area of Fig. 3.

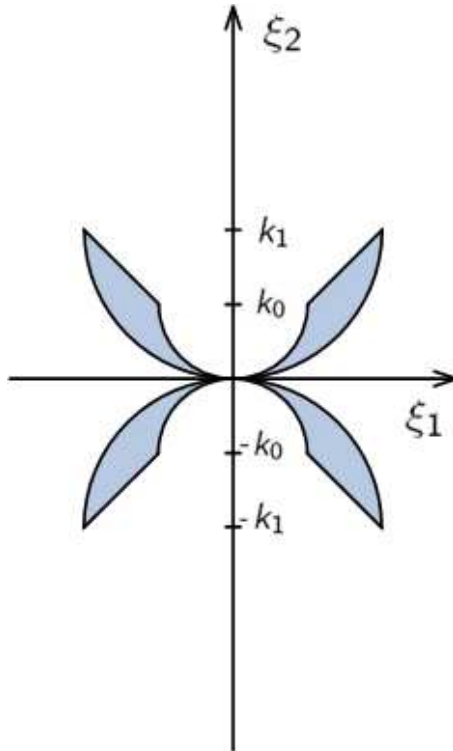


Fig. 3: Domain where \hat{f} is determined by transmission data.

Combining this with reflection measurements and assuming $k_1 = \infty$ we find that \hat{f} is determined outside the balls of radius k_0 around $(0, \pm k_0)$; see Fig. 4:

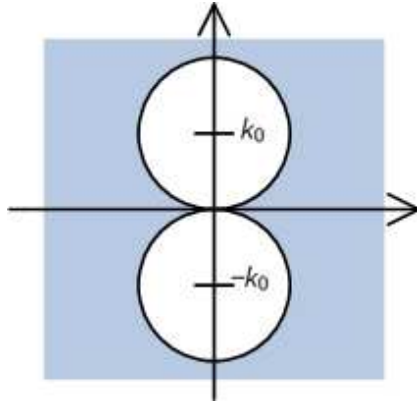


Fig. 4: Domain where \hat{f} is determined by reflection and transmission measurements.

We see that combined reflection and transmission measurements determine part of the low frequency part of \hat{f} from one downgoing plane wave, even if the source wavelet does not contain zero frequencies, i. e. $k_0 > 0$. The domain of the determined frequencies become considerably larger if we use more plane waves. For instance, if we use two plane waves making an angle of $\pi/2$ the domain where \hat{f} is not determined shrinks to four spindle shaped areas; see Fig. 5:

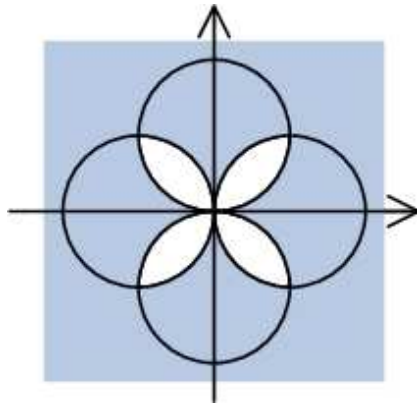


Fig. 5: Spindle shaped areas in which \hat{f} is not determined by combined reflection and transmission data from 2 orthogonal plane waves.

References

- [1] SCHULTZ, P. S. - CLAERBOUT, I. F.: Velocity estimation and downward continuation by wavefront synthesis. *Geophysics* **43**, 691 - 714 (1978).
- [2] JI, Jun: Prestack migration velocity analysis using wavefront synthesis. *SEP* **82**, 1 - 11 (2001).
- [3] NATTERER, F. and WÜBBELING, F.: *Mathematical Methods in Image Reconstruction*. SIAM, Philadelphia 2001.
- [4] BLEISTEIN, N., COHEN, I. K., and STOCKWELL, I. W.: *Mathematics of Multidimensional Seismic Imaging, Migration and Inversion*. Springer 2001.
- [5] ROSE, I. H., CHENEY, M., and DEFACIO, B.: The connection between time-frequency-domain-three dimensional inverse scattering methods. *Math. Phys.* **25**, 2995 - 3000 (1984).
- [6] VERSTEEG, R. V. and GRAU, C. (eds.): *The marmousi experience*, In: *Proc. EAEG Workshop on Practical Aspects of Seismic Data Inversion* (1990).
- [7] NATTERER, F.: *Numerical solution of bilinear inverse problems*, Technical Report **19/96**, Fachbereich Mathematik der Universität Münster (1996).
- [8] FINK, M.: Time reversal of ultrasonic fields - part 1: basic principles, *IEEE Transactions on Ultrasonics, Ferroelectrics, and Frequency Control*, **39**, 555-566 (1992).
- [9] SIELSCHOTT, H.: *Rückpropagationsverfahren für die Wellengleichung in bewegtem Medium*. Dissertation, Münster 2000.
- [10] NATTERER, F., SIELSCHOTT, H. and DERICKS, W.: *Schallpyrometric*. In: Hoffmann, K. H. et al. (eds.): *Mathematik - Schlüsseltechnologie der Zukunft*. Springer, 1997.
- [11] SYMES, W. W.: *Mathematics of Seismic Imaging*. C.I.M.E. Short Course, Martina Franca, September 2002.

- [12] HERMAN, G. T.: Image Reconstruction from Projections: The Fundamentals of Computerized Tomography. Academic Press, 1980.
- [13] DIERKES, T., DORN, O., NATTERER, F., Palamodov, V. and Sielschott, H.: Fréchet derivatives for some bilinear inverse problems, SIAM J. Appl. Math. **62**, 2092-2113 (2002).
- [14] BUNKS, C., SALECK, F. M., ZALESKI, S., and CHAVENT, G.: Multiscale seismic waveform inversion, Geophysics, **60**, 1457-1473 (1995).
- [15] NATTERER, F.: An algorithm for 3 D ultrasound tomography. In: Chavent, G., Sabatier, P.C. (eds.): Inverse Problems of Wave Propagation and Diffraction, Springer (1997).